Journal of Electronics, Electromedical Engineering, and Medical Informatics
Multidisciplinary : Rapid Review : Open Access Journal eISSN: 2656-8632

RESEARCH ARTICLE OPEN ACCESS

Manuscript received May 18, 2022; revised June 20, 2022; accepted July 10, 2022; date of publication July 29, 2022
Digital Object Identifier (DOI): https://doi.org/10.35882/jeeemi.v4i3.249

Analysis of the Geiger Muller Ability on the Effect of Collimation Area and Irradiation Distance on the Dose of X-Ray Machine Measurements

Wahyu Pratama[1], M.Ridha Mak'ruf [1], Tri Bowo Indrato [1], Endro Yulianto [1], Lamidi [1], Maduka Nosike[2] and Sambhrant Srivastava[3]

[1] Department of Medical Electronics Technology, Poltekkes Kemenkes Surabaya, Indonesia
[2] Federal University Gusau, Nigeria
[3] APJ Abul Kalam Technical University, India

[#]**Corresponding author:** M. Ridha Mak'ruf (ridha@poltekkesdepkes-sby.ac.id)

ABSTRACT Radiation cannot be felt directly by the five human senses. For the occupational safety and security, a radiation worker or radiographer is endeavored to receive radiation dose as minimum as possible, which is by monitoring the radiation using a radiation measuring device. The purpose of this study was to analyze the effect of collimation area and irradiation distance on x-ray dose measurement using Geiger Muller. In this case, the author tried to make a dosimeter by using the Muller Geiger module and displayed it on a personal computer. This research employed Muller Geiger sensor to detect X-ray dose and velocity, Arduino for data programming, Bluetooth HC-05 for digital communication tool between hardware and personal computer, and personal computer to display the reading. Current research was conducted using Pre-Experimental research design. Based on the results of data collection and comparison with the standard tool, it can be concluded that the greater the tube current setting (mA), the greater the dose and rate of radiation exposure at a distance of 100cm with 50KV and 70KV settings, and a distance of 150cm with 50KV settings. However, it is inversely proportional to the measurement results at a distance of 150cm with a 70KV setting. The results of this study are further expected to determine the ability of Geiger Muller to measure the dose to the irradiation distance or collimation area and can be used as a reference for further research in this field.

INDEX TERMS Radiation, Geiger Muller, Arduino

I. INTRODUCTION

Technology has been developing in various fields, especially in the field of radiology. However, human being still has the limitation of being incapable in detecting the presence of radiation [1][2][3]. Radiation is something that cannot be seen, felt or known to exist [4]. In this case, ionizing radiation is a type of radiation that is widely used in the field of radiodiagnostics using x-ray device radiation sources, which are further used for various medical purposes such as X-rays [3][5][6][7]. In occupational safety, a radiation worker or radiographer is encouraged to receive the radiation dose as minimum as possible, namely by monitoring the radiation using a radiation gauge [8][9].

The output results of the X-ray device are very important in order to know whether the value obtained is in accordance with the setting made by radiographer or there is a difference or even deviation of the value from the setting determined [10][11][12]. Therefore, conformity test on the results of the X-ray device output was carried out to obtain the actual value, thus the patient will not receive excessive X-ray exposure [13][14]. This conformity test activity needs a testing tool that is often used by BAPETEN personnel to find out how much the output value of KV, Time, Dose, Room leak, mA, and mAs

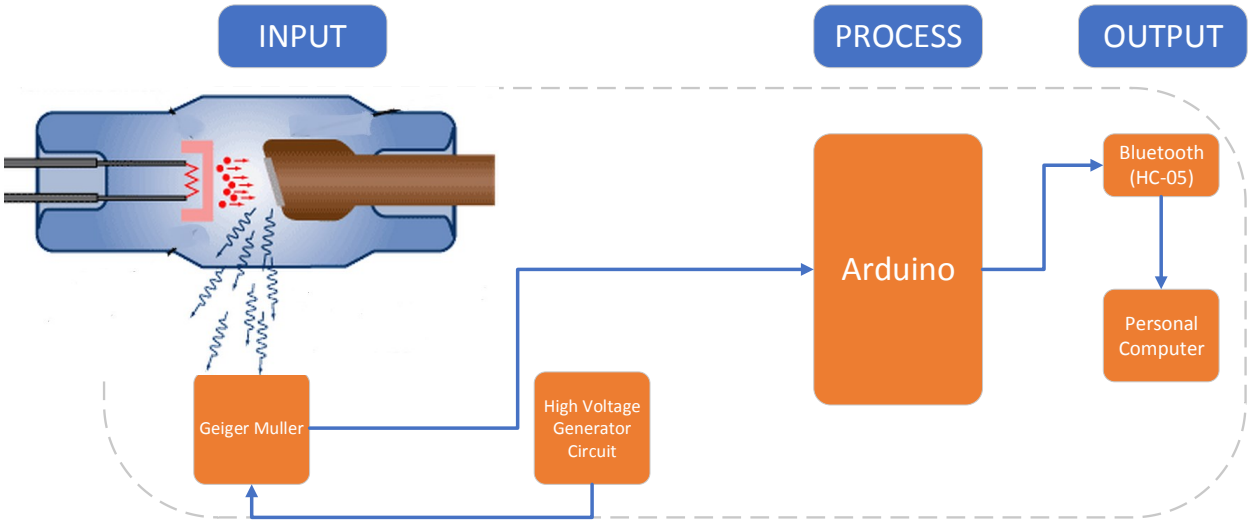

FIGURE 1. **X-ray dose measurement using the Geiger Muller sensor. After the data is processed on the Arduino, the data will be displayed on the Personal Computer via the bluetooth interface**

from an X-ray device unit [15][16][17]. We hereby wanted to conduct analysis based on previous research and develop the study by adding the Geiger Muller sensor to measure the radiation doses. Researchers previously experienced constraints or difficulties during data collection at 50-60KV [18], so in this case, we analyzed the factors affecting the performance effectiveness of both sensors by looking at the influence of the collimation or the irradiation. Furthermore, this research is expected to find out the ability of Geiger Muller to measure the doses against the irradiation distance and collimation area [19].

In 2012, research was carried out by Ivan Morales, Andres Monterroso, and Silvio Urizar discussing the design, manufacture, and calibration of Geiger Muller based on microcontroller. During the calibration, Muller's Geiger tube exceeded the expected dose rate detection range. In that case, the datasheet showed its maximum value was 30 [uR/s] (100 [uSv/h]), but during the calibration, the device had a linear response of up to 200 [uSv/h] [20]. Therefore, for a steady shift in a high-voltage tube, it had to be modified to produce an accurate one. The researchers stated that the accuracy of radiation measurements using the Geiger Muller detector was 90.71% for radiation measurements in a closed room, but the distance in the measurements was unknown [21]. Dosing has an association with the extent of copolylation. In studies using x-ray fluoroscopy devices, if collimation is maximized, it can reduce the dose received by the patient [22][23][24]. However, if it is inversely proportional to the relationship of the distance between the x-ray source and the patient, it does not significantly affect the dose received [21][25].

This study aimed to determine the limits on how far and how wide the collimation area for Scintillator and Geiger Muller. When the distance and collimation area were set, the effectiveness of Scintillator and Geiger Muller in optimally working can be assessed. After that, the research was also expected to determine the ability of Geiger Muller to measure the dose to the irradiation distance and collimation area. Based on the previous literature, the collection of Tube Voltage, Time, and Dose data has never been done for the irradiation distance and collimation area of general X-ray device [26][27][28]. This data collection aimed to determine the limit of the distance and collimation area for Scintillator and Geiger Muller. In this case, the distance and area of the collimation were assessed for to which extent the Scintillator and Geiger Muller can work optimally. Furthermore, the purpose of this study was to analyze the influence of collimation area and irradiation distance on x-ray machine dose and velocity measurements using Geiger Muller. With this research, it is expected that the ability of Geiger Muller to measure the dose to the irradiation distance and collimation area can be obtained, so that this study can be used as a reference for future researchers.

II. MATERIALS AND METHODS

A. DATA COLLECTION

In this study, measurement analysis was performed on a 30x30 cm, 20x20cm, and 10x10cm area at distances of 100cm and 150cm using Geiger Muller module.

1) MATERIALS AND TOOL

This research used Geiger Muller (with specifications of Ray 20mR/hour~120mR/hour, Ray in the range of 100~1800, changing Index/minute·CM2 soft Ray Detection of beta and gamma radiation) as the radiation counter, Arduino UNO as the microcontroller and Arduino software for data processing and programming, as well as 16x2 character LCD and Personal Computer for display. Meanwhile, in order to send the data from the microcontroller to the personal computer employed, this research used Bluetooth HC-05.

2) EXPERIMENT

In this study, measurements were carried out 5 times at each setting (50KV, 200mA, 500mS; 50KV, 400mA, 500mS; 70KV, 100mA, 500mS; and 70KV, 160mA, 500mS) and each distance (100cm and 150cm) in the predetermined collimation area (10cm x 10cm, 20cm x 20cm, 30cm x 30cm). Then, it was compared using a comparison tool, namely a dosimeter. FIGURE 1 shows the diagram block of this study. Basically, Arduino as data processing comes from the Geiger Muller and HV Series generator. The dosing data are then sent by bluetooth HC-05 and displayed on the Personal Computer, while X-rays are captured by Geiger Muller. The potential difference in the anode detector and Geiger Muller cathode give rise to an electric field so that a pair of electron ions get a considerable addition of kinetic energy. Then, there is a negative and positive ions separation event. When the detector detects filled radiation entering through the tube window, electrons will move towards the detector cathode to produce current, a frequency counter voltage proportional to the intensity of the radiation received. The detector's output voltage is then entered and processed by arduino. The results of the scaffolding are then processed by converting each voltage counter then multiplied by one minute, so that the number of counters is calculated in one minute or called CPM (Count per Minute). CPM is then converted to a unit of value of µSv (MicroSievert) by multiplying the CPM result by the conversion factor of the tube type used to produce output in mR (milliRontgen) units. Furthermore, the data that have been processed by arduino will be sent by bluetooth HC-05 and displayed on the Personal Computer. FIGURE 2 shows the geiger muller module used in this study.

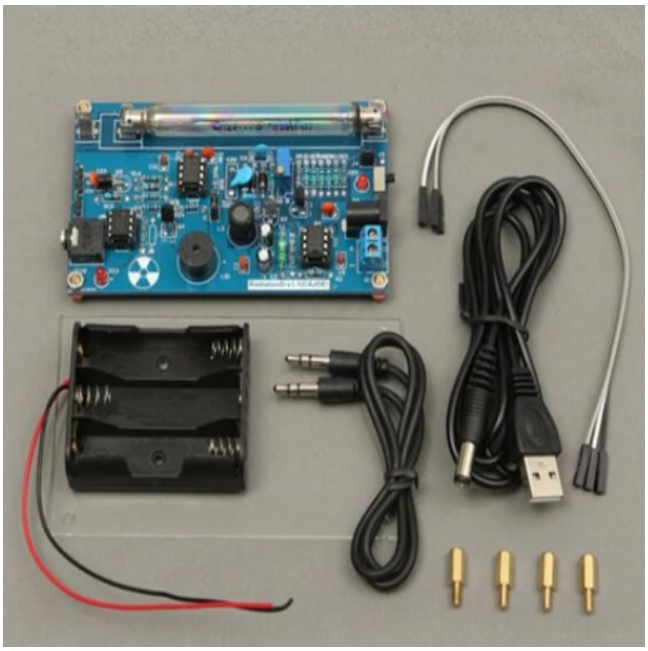

FIGURE 2 Geiger Muller Sensor Module used to receive X-ray radiation

The figure above is the geiger muller sensor module used in this study.

FIGURE 3 shows the flowchart of this study, in which, when the device is turned on, muller's Geiger sensor works. Then, the sensor can read the radiation from the x-ray machine. In this case, the user connects the tool to the Personal Computer. If the data are not received, instructions will appear to carry out re-connect. If the data can be received, the data will be displayed on the display.

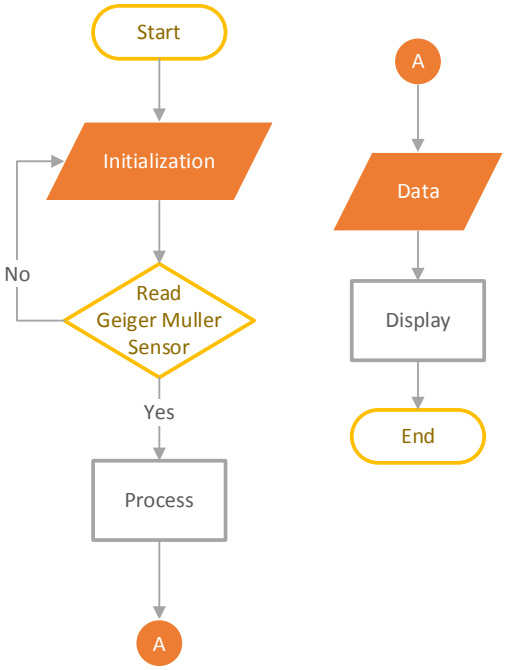

FIGURE 3 Flowchart measurement using Geiger Muller sensor for X-ray radiation measurement.

B. DATA ANALYSIS

Data analysis was carried out on every 120 data resulting from noise and air flow measurements 5 times using the following formulas.

- Mean/Average

Mean/average is the number obtained by dividing the number of data values by the number of data in the set. The following is the average formula in equation (1).

$$(\bar{X}) = \frac{\sum Xi}{n} \quad (1)$$

Based on equation (1), $\bar{X}$ represents the average, $\sum Xi$ represents the number of data values, and n represents the lots of data (1, 2, 3,..., n).

- Standard Deviation

Standard deviation is a value that indicates the level (degree) of variation in a group of data or a standard measure of deviation from the mean. The following is the standard deviation formula in equation (2).

$$SD = \sqrt{\frac{\sum_{i=1}^{n}(Xi-\bar{X})^2}{(n-1)}} \quad (2)$$

Based on equation (2), SD represents the standard deviation, Xi represents the data value, $\bar{X}$ represents the mean or average, and n represents lots of data.

- Uncertainty

Uncertainty type A is the uncertainty resulting from the statistic calculations. The following equation (3) is the formula for uncertainty type A.

$$UA = \frac{SD}{\sqrt{n}} \quad (3)$$

Based on equation (3), SD represents the standard deviation and n indicates lots of data.

- Error (%)

Error is the result of the calculated value due to the smallest scale value, calibration error, changes in the value of measurement parameters and the environment. Therefore, the measurement can be disturbed, since it is difficult to get the actual value. The following equation (4) is the error formula.

$$\%Error = \frac{(Xn-\bar{X})}{\bar{X}}\ x\ 100\% \quad (4)$$

Based on equation (4), the error is in percentage with Xn represents the measured value and $\bar{X}$ represents the average setting value.

III. RESULT

FIGURE 4 shows the results of the module in this study. The following figure is an entire tool module. It consists of Geiger Muller module as an X-ray radiation detector, arduino nano as the center for data programming and processing, bluetooth HC-05 for digital communication between hardware and Personal Computer, lithium batteries as a tool voltage supply, and charger modules to charge the batteries.

FIGURE 4 The entire measurement module using Geiger Muller sensor for X-ray radiation measurement.

FIGURE 5 shows the entire schematics circuit consisting of several components including Geiger Muller, Arduino Nano, Battery, Bluetooth HC-05, and LCD.

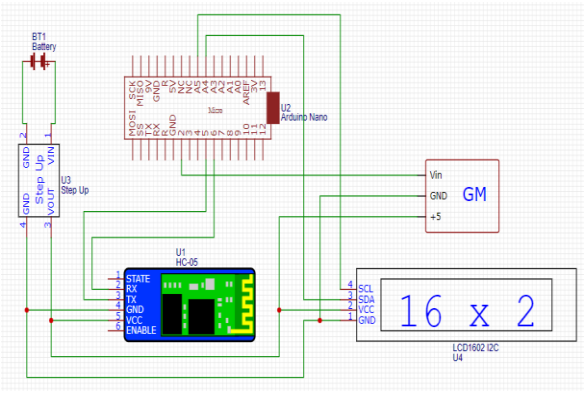

FIGURE 5 The entire measurement schematics using Geiger Muller sensor for X-ray radiation measurement.

A. MEASUREMENT RESULT WITH STANDARD DOSIMETRY

In this research, measurements were carried out 5 times at each setting (50KV, 200mA, 500mS; 50KV, 400mA, 500mS; 70KV, 100mA, 500mS; and 70KV, 160mA, 500mS) and each distance (100cm and 150cm) at collimation area (10cm x 10cm, 20cm x 20cm, 30cm x 30cm). After that, it was compared with a comparator device that is a dosimeter.

TABLE 1
Measurement results of Dose and Velocity of Radiation Comparison with 100cm Irradiation Distance (50KV, 200mA, and 500mS)

Dose	Collimation wide	Mean	
		Module	Dosimetry
mGy	10x10	2.16	2.12
	20x20	2.18	2.13
	30x30	2.20	2.21
mGy/s	10x10	4.35	4.18
	20x20	4.42	4.28
	30x30	4.47	4.43

Based on table above, the largest dose error percentage value obtained in the area of 20x20 collimation was 2.13% with a correction value of 0.05 mGy. The value of the largest percentage of radiation exposure rate at the area of 10x10 concentration was 4.05% with a correction value of 0.17 mGy/s. Meanwhile, the smallest dose error percentage in the area of 30x30 concentration was 0.36% with a correction value of 0.01 mGy and the percentage error value of the smallest radiation exposure rate at a concentration area of 30x30 was 0.95% with a correction value of 0.04 mGy/s.

TABLE 2
. Measurement results of Dose and Velocity of Radiation Comparison with 100cm Irradiation Distance (50KV, 400mA, and 500mS)

Dose	Collimation wide	Mean	
		Module	Dosimetry
mGy	10x10	4.07	4.24
	20x20	4.08	4.42
	30x30	3.91	4.50
mGy/s	10x10	7.42	8.48
	20x20	8.84	8.84
	30x30	8.52	9.01

Based on the table above, the largest dose error percentage value obtained in the area of 30x30 concentration was 13.07% with a correction value of 0.59 mGy. Furthermore, the largest percentage of radiation exposure rate at the area of 10x10 concentration was 12.41% with a correction value of 1.05 mGy/s. Meanwhile, the smallest dose error percentage at the 10x10 concentration area was 3.87% with a correction value of 0.16 mGy and the percentage error of the smallest radiation exposure rate at the 20x20 concentration area was 0.00% with a correction value of 0.00 mGy/s.

TABLE 3.
Measurement results of Dose and Velocity of Radiation Comparison with 100cm Irradiation Distance (70KV,100mA, and 500mS)

Dose	Collimation wide	Mean	
		Module	Dosimetry
mGy	10x10	2.16	2.36
	20x20	2.19	2.40
	30x30	2.24	2.46
mGy/s	10x10	4.31	4.73
	20x20	4.37	4.80
	30x30	4.48	4.93

Based on the table above, the largest dose error percentage obtained in the area of 30x30 concentration was 8.79% with a correction value of 0.22 mGy. Furthermore, the the largest percentage value of radiation exposure rate at the area of 30x30 concentration was 9.01% with a correction value of 0.44 mGy/s. Meanwhile, the smallest dose error percentage in the 10x10 concentration area was 8.49% with a correction value of 0.20 mGy and the percentage error value of the smallest radiation exposure rate at a 10x10 concentration area was 8.84% with a correction value of 0.42 mGy/s.

TABLE 4.
Measurement results of Dose and Velocity of Radiation Comparison with 100cm Irradiation Distance (70KV, 160mA, and 500mS)

Dose	Collimation wide	Mean	
		Module	Dosimetry
mGy	10x10	3.58	3.74
	20x20	2.11	3.86
	30x30	1.92	3.94
mGy/s	10x10	7.22	7.48
	20x20	7.36	7.71
	30x30	7.00	7.88

Based on the table above, the largest dose error percentage obtained in the area of 30x30 concentration was 51.14% with a correction value of 2.01 mGy. Furthermore, the largest percentage value of radiation exposure rate at a concentration area of 30x30 was 11.14% with a correction value of 0.88 mGy/s. Meanwhile, the smallest dose error percentage at the 10x10 concentration area was 4.33% with a correction value of 0.016 mGy and the percentage error value of the smallest radiation exposure rate at a 10x10 concentration area was 3.48% with a correction value of 0.26 mGy/s.

TABLE 5.
Measurement results of Dose and Velocity of Radiation Comparison with 150cm Irradiation Distance (50KV, 200mA, and 500mS)

Dose	Collimation wide	Mean	
		Module	Dosimetry
mGy	10x10	1.09	0.944
	20x20	1.12	0.94
	30x30	1.11	0.97
mGy/s	10x10	1.99	1.89
	20x20	1.99	1.89
	30x30	1.98	1.95

Based on the table above, the largest dose error percentage value obtained in the area of 20x20 concentration was 18.43% with a correction value of 0.17 mGy. Furthermore, the largest percentage value of radiation exposure rate in the area of 20x20 concentration was 5.30% with a correction value of 0.10 mGy/s. Meanwhile, the smallest dose error percentage in the area of 30x30 concentration was 15.08% with a correction value of 0.15 mGy and the percentage error value of the smallest radiation exposure rate at the 30x30 concentration area was 1.54% with a correction value of 0.03 mGy/s.

TABLE 6.
Measurement results of Dose and Velocity of Radiation Comparison with 150cm Irradiation Distance (50KV, 400mA, and 500mS)

Dose	Collimation wide	Mean	
		Module	Dosimetry
mGy	10x10	1.88	1.89
	20x20	1.87	1.95
	30x30	1.94	1.97
mGy/s	10x10	3.75	3.77
	20x20	3.75	3.91
	30x30	3.73	3.94

Based on the table above, the largest dose error percentage value obtained in the area of 20x20 concentration was 4.10% with a correction value of 0.08 mGy. Furthermore, the largest percentage value of radiation exposure rate in the area of 30x30 concentration was 5.48% with a correction value of 0.22 mGy/s. Meanwhile, the smallest dose error percentage in the area of 10x10 concentration was 0.95% with a correction value of 0.02 mGy and the percentage error value of the smallest radiation exposure rate at a concentration area of 10x10 is 0.48% with a correction value of 0.02 mGy/s.

TABLE 7.
Measurement results of Dose and Velocity of Radiation Comparison with 150cm Irradiation Distance (70KV, 100mA, and 500mS)

Dose	Collimation wide	Mean	
		Module	Dosimetry
mGy	10x10	1.45	1.562
	20x20	1.48	1.66
	30x30	1.43	1.71
mGy/s	10x10	2.91	3.11
	20x20	2.94	3.31
	30x30	2.88	3.41

Based on the table above, the largest dose error percentage value obtained at the area of 30x30 concentration

was 16.14% with a correction value of 0.28 mGy. Furthermore, the largest percentage value of radiation exposure rate at a concentration area of 30x30 was 15.66% with a correction value of 0.53 mGy/s. Meanwhile, the smallest dose error percentage at the 10x10 concentration area was 6.91% with a correction value of 0.11 mGy and the percentage error value of the smallest radiation exposure rate at a 10x10 concentration area of 6.49% with a correction value of 0.20 mGy/s.

TABLE 8.
Measurements results of Dose and Velocity of Radiation Comparison with 150cm Irradiation Distance (70KV, 160mA, and 500mS)

Dose	Collimation wide	Mean	
		Module	Dosimetry
mGy	10x10	1.02	1.12
	20x20	1.62	1.38
	30x30	2.57	3.48
mGy/s	10x10	1.88	2.75
	20x20	2.22	2.67
	30x30	3.48	4.06

Based on the table above, the largest dose error percentage value obtained at the area of 30x30 concentration was 26.12% with a correction value of 0.91 mGy. Furthermore, the largest percentage value of radiation exposure rate at a concentration area of 10x10 was 31.78% with a correction value of 0.87 mGy/s. Meanwhile, the smallest dose error percentage in the area of 10x10 concentration was 8.90% with a correction value of 0.10 mGy and the percentage error value of the smallest radiation exposure rate at a concentration area of 30x30 was 14.38% with a correction value of 0.58 mGy/s.

B. COMPARISON GRAPHIC

The comparison graphic (dose) is shown in the FIGURE 6, while the velocity of radiation is shown in the FIGURE 7. at Sett 50KV and 100cm distance.

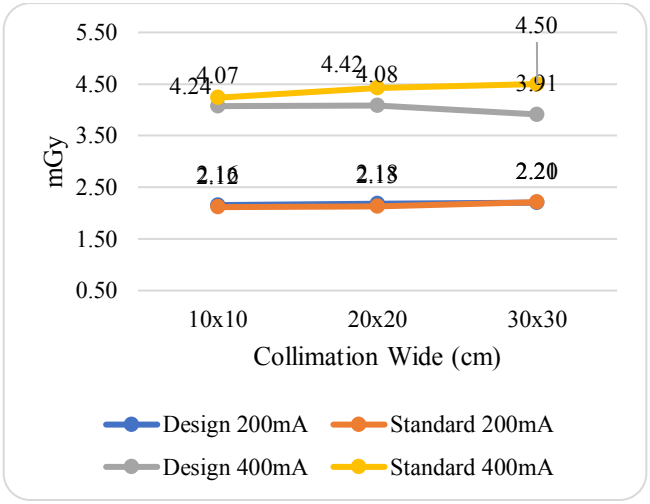

FIGURE 6. The line chart shows the Radiation Dose Reading Comparison Graph (50KV,100cm)

FIGURE 6 shows that the dose measured in the comparison module and dosimeter at 400mA is greater than the 200mA tube current setting. This means that the greater the tube current (mA), the greater the radiation produced by an X-ray machine.

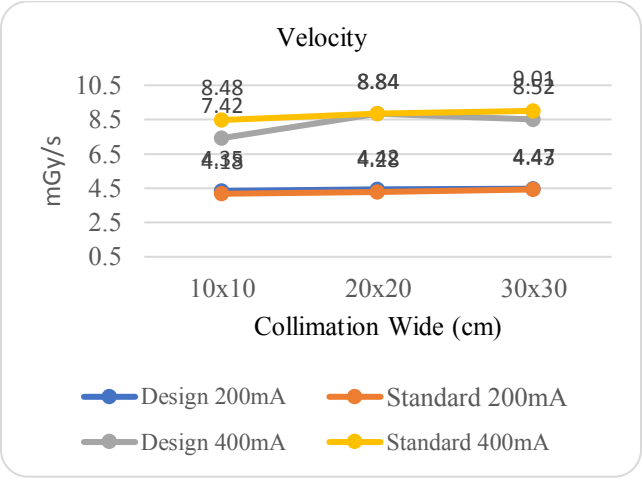

FIGURE 7. The line chart shows the Radiation Velocity Reading Comparison Graph (50KV,100cm)

FIGURE 7 shows that the radiation exposure rate measured on the comparison module and dosimeter at 400mA is greater than the tube current setting of 200mA. This indicates that the greater the tube current (mA), the greater the rate of radiation exposure produced by an X-ray machine.

Comparison graphic (dose) is shown in the FIGURE 8, while the velocity of radiation is shown in the FIGURE 9 at the setting of 70KV and 100cm distance.

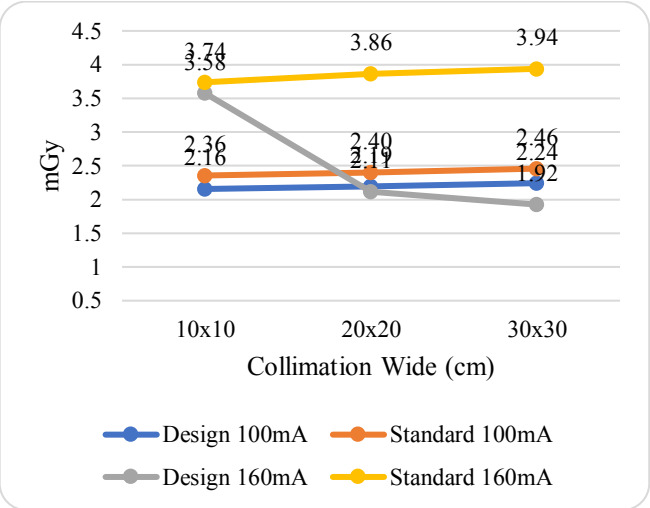

FIGURE 8. The line chart shows the Radiation Dose Reading Comparison Graph (70KV,100cm)

FIGURE 8 shows that the radiation dose measured in the comparator with the tube current setting of 160mA is greater than 100mA. However, on the module with the 160mA, the setting the dose read is not greater than the tube current setting of 100mA at a collimation area of 20x20cm and 30x30cm.

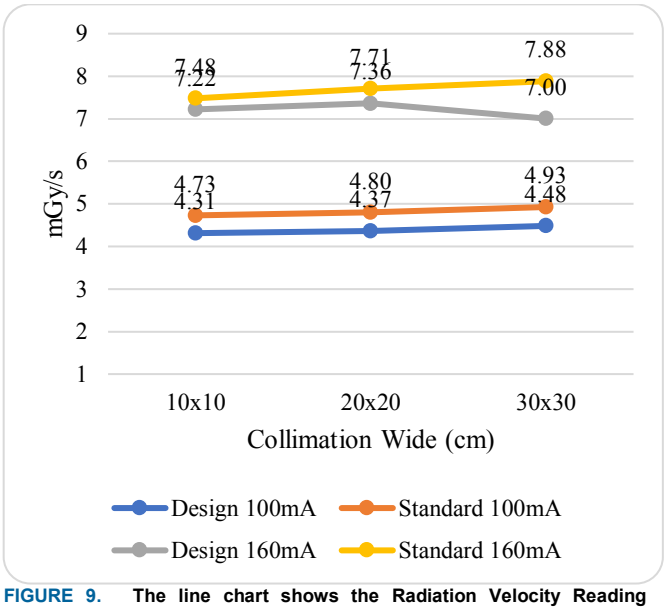

FIGURE 9. The line chart shows the Radiation Velocity Reading Comparison Graph (70KV,100cm)

FIGURE 9 shows that the radiation exposure rate measured in the comparison module and dosimeter at 160mA is greater than the tube current setting of 100mA. This means that the greater the tube current (mA), the greater the rate of radiation exposure produced by an X-ray machine.

The comparison graphic (dose) is shown in the FIGURE 10, while the velocity of radiation is shown in the FIGURE 11 at the setting of 50KV and 150 cm distance.

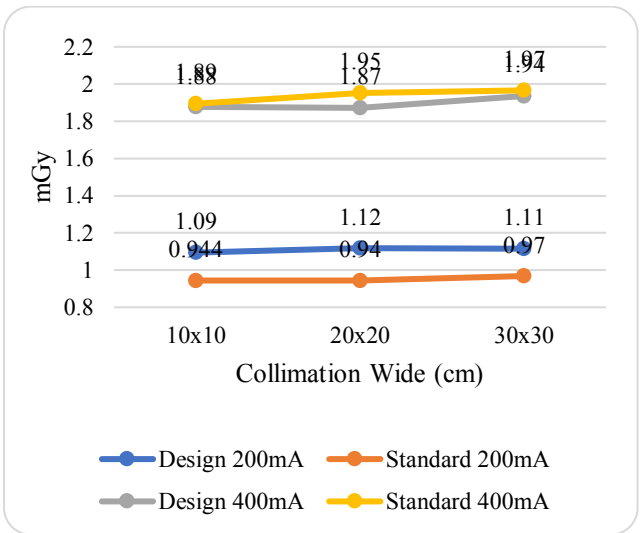

FIGURE 10. The line chart shows the Radiation Dose Reading Comparison Graph (50KV,150cm)

FIGURE 10 shows that the dose measured on the module and comparison dosimeter at 400mA is greater than the 200mA tube current setting. This means that the greater the tube current (mA), the greater the radiation produced by an X-ray machine.

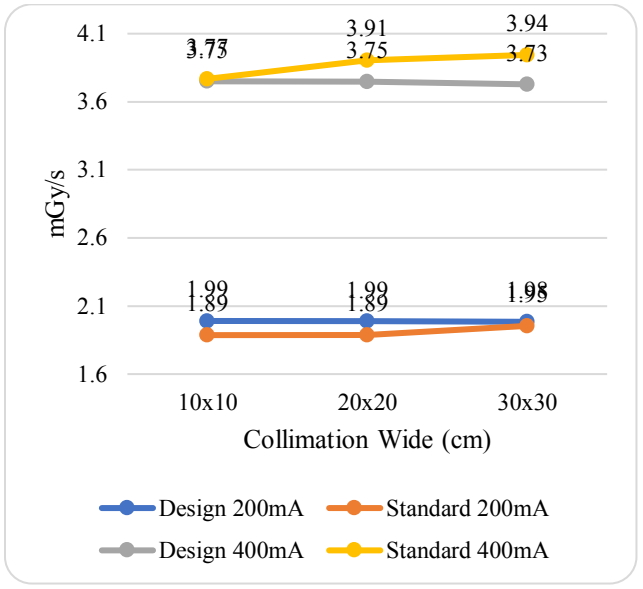

FIGURE 11. The line chart shows the Radiation Velocity Reading Comparison Graph (50KV, 150cm)

FIGURE 11 shows that the radiation exposure rate measured on the comparison module and dosimeter at 400mA is greater than the tube current setting of 200mA. This means that the greater the tube current (mA), the greater the rate of radiation exposure produced by an X-ray machine.

Comparison graphic (dose) is shown in the FIGURE 12, while the velocity of radiation is shown in the FIGURE 13 at the setting of 70KV and 150cm distance.

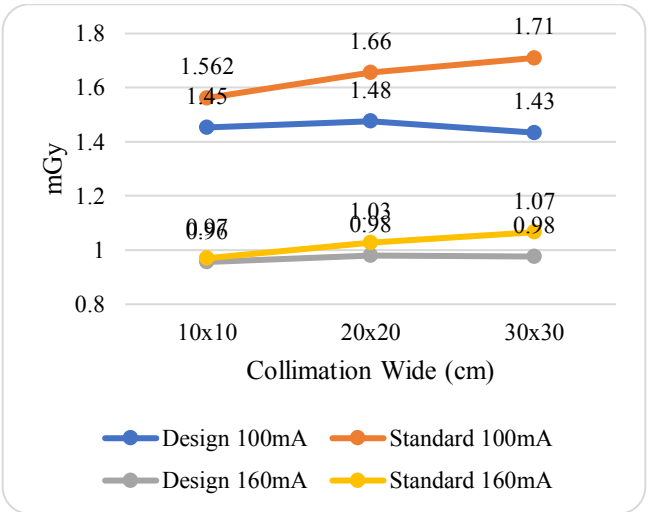

FIGURE 12. The line chart shows the Radiation Dose Reading Comparison Graph (70KV,150cm)

FIGURE 12 shows that the dose measured on the comparison module and dosimeter at 100mA is greater than the tube current setting of 160mA. This means that the greater the tube current (mA), the smaller the radiation dose produced by an X-ray machine.

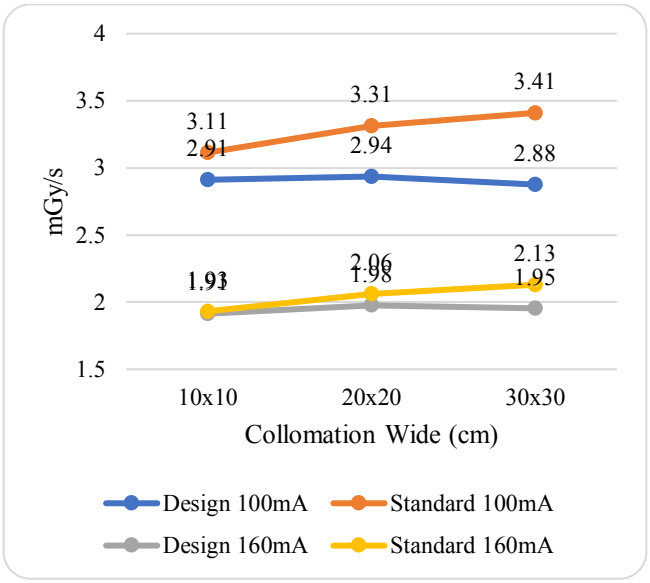

FIGURE 13. The line chart shows the Radiation Velocity Reading Comparison Graph (70KV,150cm)

FIGURE 13 shows that the radiation exposure rate measured in the comparison module and dosimeter at 100mA was greater than the 160mA tube current setting. This means that the greater the tube current (mA), the smaller the radiation exposure rate produced by an X-ray machine.

IV. DISCUSSION

The dosimetry design has been thoroughly examined and tested in this study. This has been carried out based on the dose measurement and radiation measurement velocity at each setting (50KV, 200mA, 500mS; 50KV, 400mA, 500mS; 70KV, 100mA, 500mS; and 70KV, 160mA, 500mS) and each distance (100cm and 150cm) in the collimation area (10cm x 10cm, 20cm x 20cm, 30cm x 30cm) using a comparison tool of a dosimeter.

The results of the module measurement at a distance of 100cm with the settings of 70KV, 160mA, and 500mS show that the dose read is not greater than the current setting of 100mA tube at a density of 20x20cm and 30x30cm. Meanwhile, the measurement results with the ratio of the larger the tube current (mA) of the dosimeter shows greater dose produced. In this case, the larger the tube current setting (mA), the greater the dose and rate of radiation exposure at a distance of 100cm at 50KV and 70KV settings, and at a distance of 150cm to 50KV setting. However, it is inversely proportional to the measurement results at a distance of 150cm and 70KV setting.

In this study, the results of dose measurements and radiation measurements were obtained at a distance of 100 cm and 150 cm, with several collimation area settings (10cm x 10cm, 20cm x 20cm, 30cm x 30cm). In this study, there were more variations that can complement or improve the previous research results [18][19][20].

However, this research is limited to 4 settings of voltage KV, current mA, time mS, and 3 collimation area which arguably needs to be further developed in order to get more variations in measurements so that more complex data analysis can be carried out.

V. CONCLUSION

The purpose of this study is to analyze the influence of collimation and irradiation distance on x-ray machine dose and velocity measurements using Geiger Muller. The wider the collimation, the greater the dose produced by an X-ray aircraft. In this case, the results of dose and rate measurements at a distance of 100cm are greater than the measurement at a distance of 150cm. In order to improve this research, some modifications can be done such as, modifying both hardware and software so that the measurement of dose and rate of radiation exposure is in accordance with the comparison/ calibrator and increasing the distance, tube voltage setting (KV) and current tube (mA) to get better data results and analysis. For the future work, it is expected to make modifications to both hardware and software so that the measurement of radiation dose and exposure rate is in accordance with the comparison/ calibrator and increase the distance, tube voltage setting (KV) and tube current (mA). To obtain more complex data analysis, variations in the settings of KV, mA, mS, and collimation area can be carried out as well.

REFERENCES

[1] C. A. Miller, S. D. Clarke, and S. A. Pozzi, "Effects of Detector Cell Size on Dose Rate Measurements using Organic Scintillators," *2017 IEEE Nucl. Sci. Symp. Med. Imaging Conf. NSS/MIC 2017 - Conf. Proc.*, pp. 2–4, 2018, doi: 10.1109/NSSMIC.2017.8532804.

[2] N. A. Abd Rahman *et al.*, "GSM module for wireless radiation monitoring system via SMS," *IOP Conf. Ser. Mater. Sci. Eng.*, vol. 298, no. 1, 2018, doi: 10.1088/1757-899X/298/1/012040.

[3] N. H. Wijaya, Budimansyah, and D. Sukwono, "Wireless X-ray Machine Control Based on Arduino with Kv Parameters," *J. Phys. Conf. Ser.*, vol. 1430, no. 1, 2020, doi: 10.1088/1742-6596/1430/1/012040.

[4] D. Tisseur *et al.*, "Performance evaluation of several well-known and new scintillators for MeV X-ray imaging," *2018 IEEE Nucl. Sci. Symp. Med. Imaging Conf. NSS/MIC 2018 - Proc.*, pp. 1–3, 2018, doi: 10.1109/NSSMIC.2018.8824663.

[5] A. (US) Allen B. Wright, Tucson, AZ (US); Eddy J. Peters, Tucson, "Nuclear Detection Via A System Of Widely Distributed Low Cost Detectors Having Data Including Gamma Intensities, Time Stamps And Geo-Positions," *Syst. Method Sel. Transm. Images Interes. To a User*, vol. 1, no. 12, pp. 1–4, 2002.

[6] B. Bilki, Y. Onel, E. Tiras, J. Wetzel, and D. Winn, "Development of Radiation-Hard Scintillators and Wavelength-Shifting Fibers," *2018 IEEE Nucl. Sci. Symp. Med. Imaging Conf. NSS/MIC 2018 - Proc.*, pp. 2018–2021, 2018, doi: 10.1109/NSSMIC.2018.8824541.

[7] A. S. Voyles *et al.*, "Excitation functions for (p,x) reactions of niobium in the energy range of Ep = 40–90 MeV," *Nucl. Instruments Methods Phys. Res. Sect. B Beam Interact. with Mater. Atoms*, vol. 429, pp. 53–74, 2018, doi: 10.1016/j.nimb.2018.05.028.

[8] T. E. Walters, P. M. Kistler, J. B. Morton, P. B. Sparks, K. Halloran, and J. M. Kalman, "Impact of collimation on radiation exposure during interventional electrophysiology," *Europace*, vol. 14, no. 11, pp. 1670–1673, 2012, doi: 10.1093/europace/eus095.

[9] D. Magalotti, P. Placidi, M. Dionigi, A. Scorzoni, L. Bissi, and L. Servoli, "A wireless personal sensor node for the Dosimetry of Interventional Radiology operators," *2015 IEEE Int. Symp. Med. Meas. Appl. MeMeA 2015 - Proc.*, pp. 196–201, 2015, doi: 10.1109/MeMeA.2015.7145198.

[10] L. J. Brillson, "Photoemission with Soft X-Rays," *Surfaces Interfaces Electron. Mater.*, pp. 129–145, 2012, doi: 10.1002/9783527665709.ch8.

[11] D. S. Kim, "Image Restoration for CsI(Tl)-Scintillator Mammography Detectors," *Med. Phys.*, vol. 45, no. 12, pp. 5461–5471, 2018, doi: 10.1002/mp.13218.
[12] G. K. Barends, B. Utomo, and T. B. Indrato, "Design of Instrument Measurement for X-Ray Radiation with Geiger Muller," vol. 2, no. 1, pp. 13–20, 2020.
[13] M. Bath, "Evaluating Imaging Systems : Practical Applications," *Radiat. Prot. Dosimetry*, vol. 139, no. 1, pp. 26–36, 2010.
[14] T. Grundl *et al.*, "Continuously tunable, polarization stable SWG MEMS VCSELs at 1.55 μ m," *IEEE Photonics Technol. Lett.*, vol. 25, no. 9, pp. 841–843, 2013, doi: 10.1109/LPT.2013.2250276.
[15] Dance.D.R, *Diagnostic Radiology Physics*. 2014.
[16] P. Bhattacharya *et al.*, "TlZrCl and TlHfCl Intrinsic Scintillators for Gamma Rays and Fast Neutron Detection," *IEEE Trans. Nucl. Sci.*, vol. 67, no. 6, pp. 1032–1034, 2020, doi: 10.1109/TNS.2020.2997659.
[17] P. Q. Vuong, H. J. Kim, H. Park, G. Rooh, and S. H. Kim, "Pulse shape discrimination study with Tl 2 ZrCl 6 crystal scintillator," *Radiat. Meas.*, vol. 123, pp. 83–87, 2019, doi: 10.1016/j.radmeas.2019.02.007.
[18] H. R. Fajrin, Z. Rahmat, and D. Sukwono, "Kilovolt peak meter design as a calibrator of X-ray machine," *Int. J. Electr. Comput. Eng.*, vol. 9, no. 4, pp. 2328–2335, 2019, doi: 10.11591/ijece.v9i4.pp2328-2335.
[19] D. Barclay, "IMPROVED RESPONSE OF GEIGER MULLER DETECTORS," vol. 33, no. 1, pp. 613–616, 1986.
[20] and S. U. Iv´an Morales, Member, IEEE, Andr´es Monterroso, "Design, Assembly and Calibration of a microcontroller-based Geiger-M¨uller doserate meter," no. Fig 2, pp. 1–11, 2012.
[21] J. Poletti, "The effect of source to image distance on radiation risk to the patient," *Australas. Phys. Eng. Sci. Med.*, vol. 26, no. 3, pp. 110–114, 2003, doi: 10.1007/BF03178779.
[22] A. Toda and S. Kishimoto, "X-Ray Detection Capabilities of Plastic Scintillators Incorporated with ZrO2Nanoparticles," *IEEE Trans. Nucl. Sci.*, vol. 67, no. 6, pp. 983–987, 2020, doi: 10.1109/TNS.2020.2978240.
[23] P. Press, "Protection against ionizing radiation from external sources used in medicine," *Ann. ICRP*, vol. 9, no. 1, 1982.
[24] C. C. Chen, Y. J. Liu, G. N. Sung, C. C. Yang, C. M. Wu, and C. M. Huang, "Smart electronic dose counter for pressurized metered dose inhaler," *IEEE Biomed. Circuits Syst. Conf. Eng. Heal. Minds Able Bodies, BioCAS 2015 - Proc.*, vol. 121, no. 3, p. 7234, 2015, doi: 10.1109/BioCAS.2015.7348320.
[25] H. Yu *et al.*, "Significant Enhancement in Light Output of Photonic-Crystal-Based YAG:Ce Scintillator for Soft X-Ray Detectors," *IEEE Trans. Nucl. Sci.*, vol. 66, no. 12, pp. 2435–2439, 2019, doi: 10.1109/TNS.2019.2954692.
[26] R. Malhotra and Y. B. Gianchandani, "A microdischarge-based neutron radiation detector utilizing a stacked arrangement of micromachined steel electrodes with gadolinium film for neutron conversion," *IEEE Sens. J.*, vol. 15, no. 7, pp. 3863–3870, 2015, doi: 10.1109/JSEN.2015.2397006.
[27] R. Malhotra and Y. B. Gianchandani, "A microdischarge-based neutron radiation detector utilizing sputtered gadolinium films for neutron conversion," *Proc. IEEE Sensors*, pp. 1–4, 2013, doi: 10.1109/ICSENS.2013.6688132.
[28] R. Malhotra and Y. B. Gianchandani, "A Gamma Radiation Detector With Orthogonally Arrayed Micromachined Electrodes," *J. Microelectromechanical Syst.*, vol. 24, no. 5, pp. 1314–1321, 2015, doi: 10.1109/JMEMS.2015.2394322.